Inst. Phys. Conf. Ser. No 161: Section 6
Paper presented at Electron Microscopy and Analysis Group Conf. EMAG99, Sheffield, 1999

The direct determination of magnetic induction maps from Lorentz images

C B Boothroyd and R E Dunin-Borkowski[1]

Department of Materials Science, University of Cambridge, Pembroke St, Cambridge CB2 3QZ
[1]Department of Materials, University of Oxford, Parks Road, Oxford OX1 3PH

ABSTRACT: Lorentz microscopy is a simple method by which the domain walls of magnetic materials can be made visible in a qualitative fashion. Here we describe a method whereby the magnitude and direction of magnetisation can be obtained from Lorentz images quantitatively, using NdFeB and Co as examples.

1. INTRODUCTION

Out-of-focus (or Lorentz) images of magnetic materials contain contrast from domain walls and magnetisation ripple and can be very difficult to interpret intuitively (Cohen, 1967). As a result, vector maps of magnetisation distributions in materials are usually determined using more specialised techniques such as off-axis electron holography (Tonomura, 1992) and differential phase contrast microscopy (Chapman, 1984). Here, we illustrate how two-dimensional magnetisation distributions *can* in fact be determined from Lorentz images directly. Our approach relies on the fact that in the absence of dynamical effects the intensity of a Lorentz image can be written

$$I(x) \approx 1 - (f\lambda/2\pi)(d^2\phi(x)/dx^2) + \dots \qquad (1)$$

where f is the defocus, λ is the electron wavelength and x is a distance in the plane of the sample (Cowley, 1995). Assuming that neither the mean inner potential V(x) nor the in-plane component of the magnetic induction $B_{\|}(x)$ vary in the beam direction, the electron phase

$$\phi(x) = C_E V(x)t(x) - (2\pi e/h) \int B_{\|}(x)t(x)dx \qquad (2)$$

where t(x) is the sample thickness and C_E is an energy-dependent constant (Dunin-Borkowski et al., 1998). $\phi(x)$ can be recovered by integrating I(x) twice, which is best done in Fourier space. $B_{\|}(x)$ can then be determined from $\phi(x)$. This approach is also the basis of an algorithm for recovering phases in light optics by Paganin and Nugent (1998). Experimental complications include the presence of variations in mean inner potential and amplitude (or absorption) contrast associated with sample thickness and dynamical diffraction effects. In practice, many of these artefacts can be removed by subtracting or dividing each Lorentz image by an in-focus image. The approach also necessarily enhances the low frequencies in the image, which means that any slight variations in background intensity due to thickness variations or bend contours are greatly amplified. This means that some high pass filtering of the image may be required. This filter has to be chosen with care to avoid removing information on the scale of the domain structure being observed. A further complication is that the average gradient of the phase is lost as this is determined by contrast outside the region analysed.

Fig. 1a shows a test structure containing 4 magnetic domains. The electron phase is shown in fig 1b, and simulated images for defocus values of -20 µm, 0 and +20 µm are shown in fig. 1c for 200 kV and C_S=8 m. There is very little contrast at focus, while the over and under focus images are approximately reversed in contrast. Fig. 1d shows the phase recovered from the

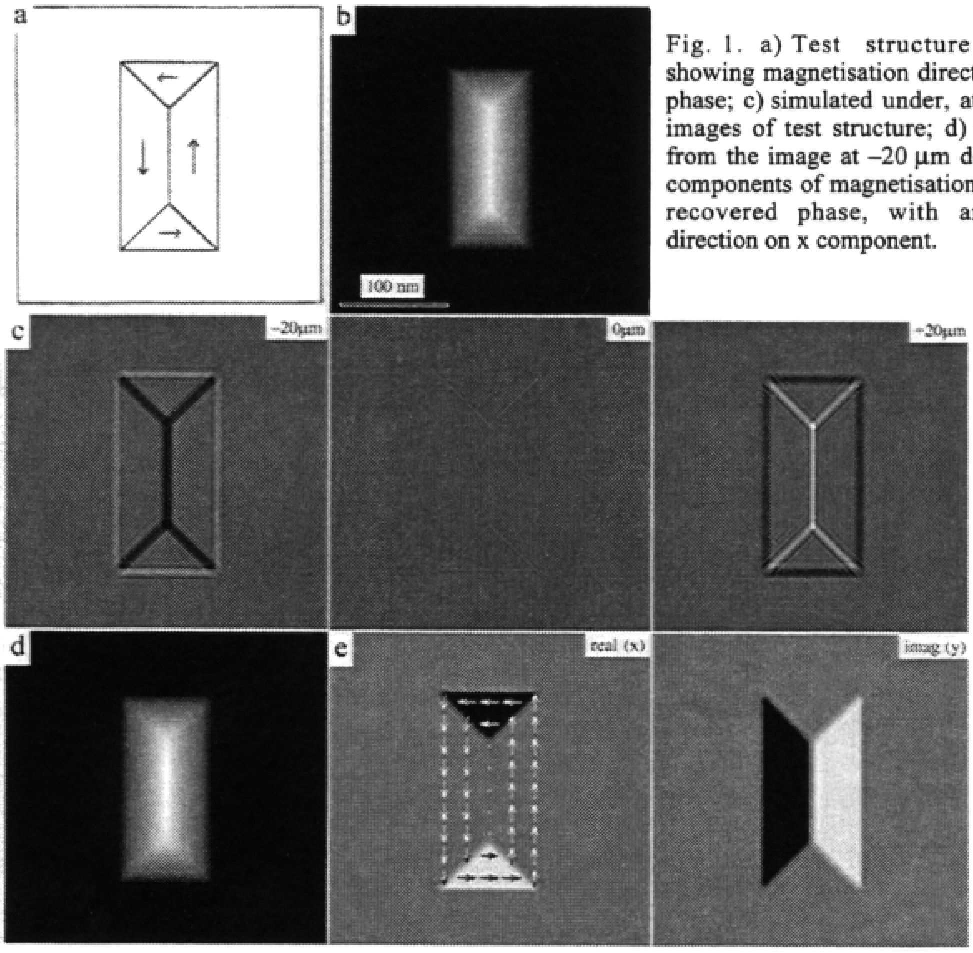

Fig. 1. a) Test structure with arrows showing magnetisation directions; b) electron phase; c) simulated under, at and over focus images of test structure; d) recovered phase from the image at –20 μm defocus; e) x & y components of magnetisation calculated from recovered phase, with arrows showing direction on x component.

–20 μm defocus image using equations (1) and (2). The recovered phase is very similar to the input phase in fig. 1b, although the resolution is slightly lower.

2. $Nd_2Fe_{14}B$

Fig. 2a shows a Lorentz image of a $Nd_2Fe_{14}B$ alloy, in which the intensity variation with specimen thickness can be treated by dividing by an in-focus image. (The Fresnel fringe at the sample edge cannot be removed in this way). The x and y components of the magnetisation, obtained by differentiating the recovered phase (fig. 2b) in the x and y directions, are shown in fig. 2c. A comparison with the magnetisation measured using holography (arrows on right image of fig. 2c) shows that the magnitude and direction of the magnetisation are recovered well. Small errors result mainly from the amplification of low frequency noise.

3. Co films

The images of thin Co films shown in fig. 3a are in principle easier to analyse than NdFeB as they are of constant thickness. The magnetic structure is also on a much finer scale, meaning that more of the low frequency noise can be filtered out. An example of the recovered magnetisation from a film about to undergo reversal is shown in fig. 3b.

The magnetisation of such a film is expected to be solely in-plane. Thus, a histogram of the x and y components of magnetisation in fig 3b (where distance from the origin represents the magnitude of the magnetisation and position represents the direction of magnetisation) forms an arc of a circle centred on the origin, as shown in fig 3c. However, the origin of the histogram lies on the brightest part of the arc and not at its centre. This means that the magnetisation is wrong by a constant amount whose x and y components are given by the centre of the arc. This magnetisation error corresponds to a constant phase ramp in the phase image from which fig 3b is derived. The error arises because only a small region of the specimen was processed, with the

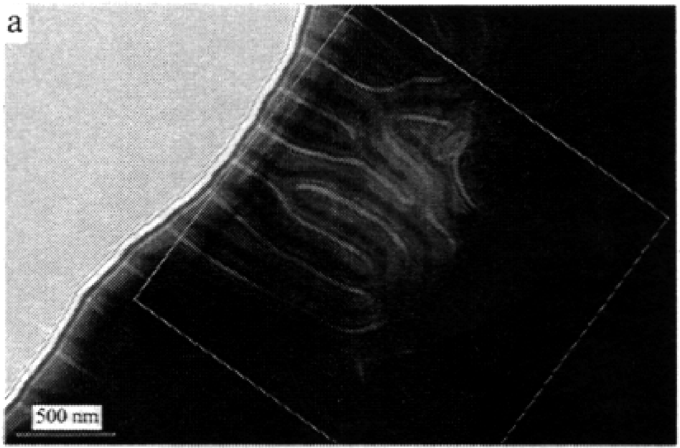

Fig. 2. a) original image; b) recovered phase from region in box in a; c) x & y components with arrows on left image from region in box in b. The arrows on the y component (right) image are the magnetisation from a hologram of the same area for comparison.

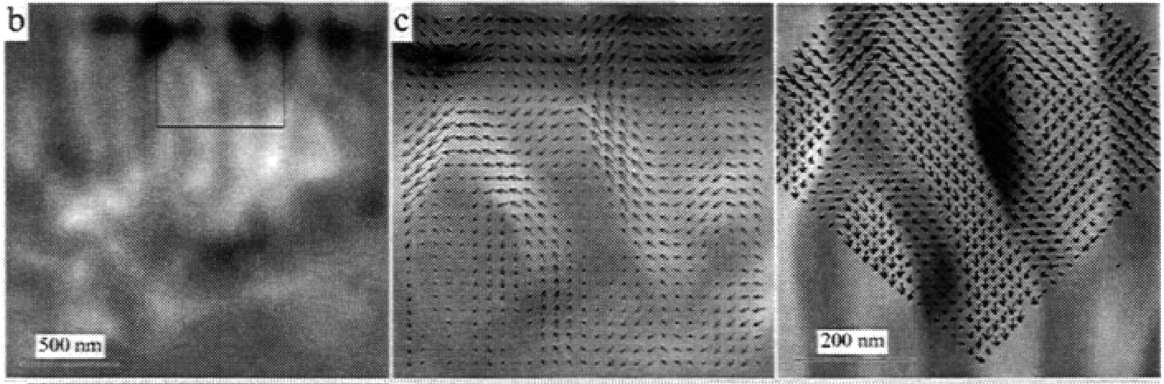

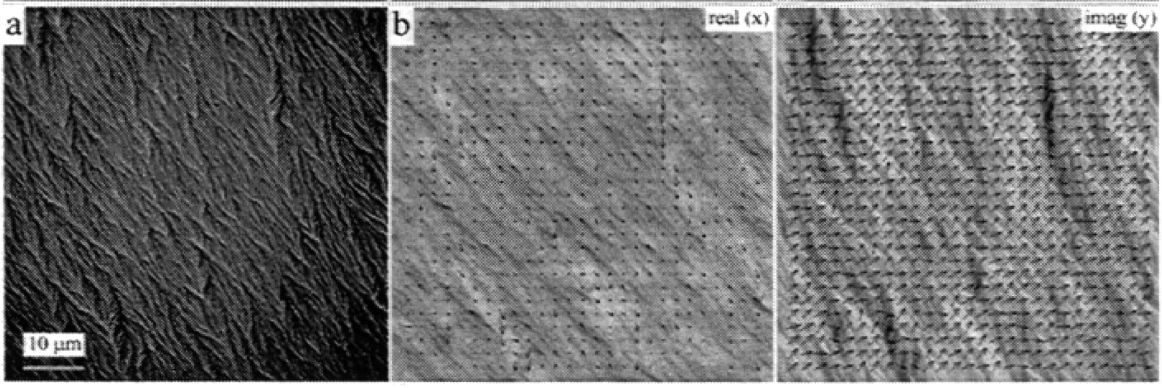

Fig. 3. a) Lorentz image of a 15 nm thick Co film within a tunnel junction (IBM Almaden) with an applied field of -2.6×10^{-3} T; b) x and y components of magnetisation recovered from a) with arrows on left image. The arrows on the right image show the magnetisation after correction. c) Histogram of x and y components of magnetisation from b with the x component horizontally, the y component vertically and the origin in the middle. Dark means higher frequency and it can be seen that the histogram forms an arc of a circle.

image contrast giving rise to the phase ramp outside the area analysed. The magnetisation after correcting for the phase ramp is shown on the right in fig 3c.

Histograms of the magnetisation can be used to give information about the distribution of magnetic domains in these Co films as the applied magnetic field is changed so as to take the film through a hysteresis cycle, as shown in fig. 4. When magnetised fully in one direction (fig. 4a) most of the domains are aligned with a small amount of spread. As a reverse field is applied the spread in domain alignment becomes larger as shown by the enlargement of the arc in fig 4b.

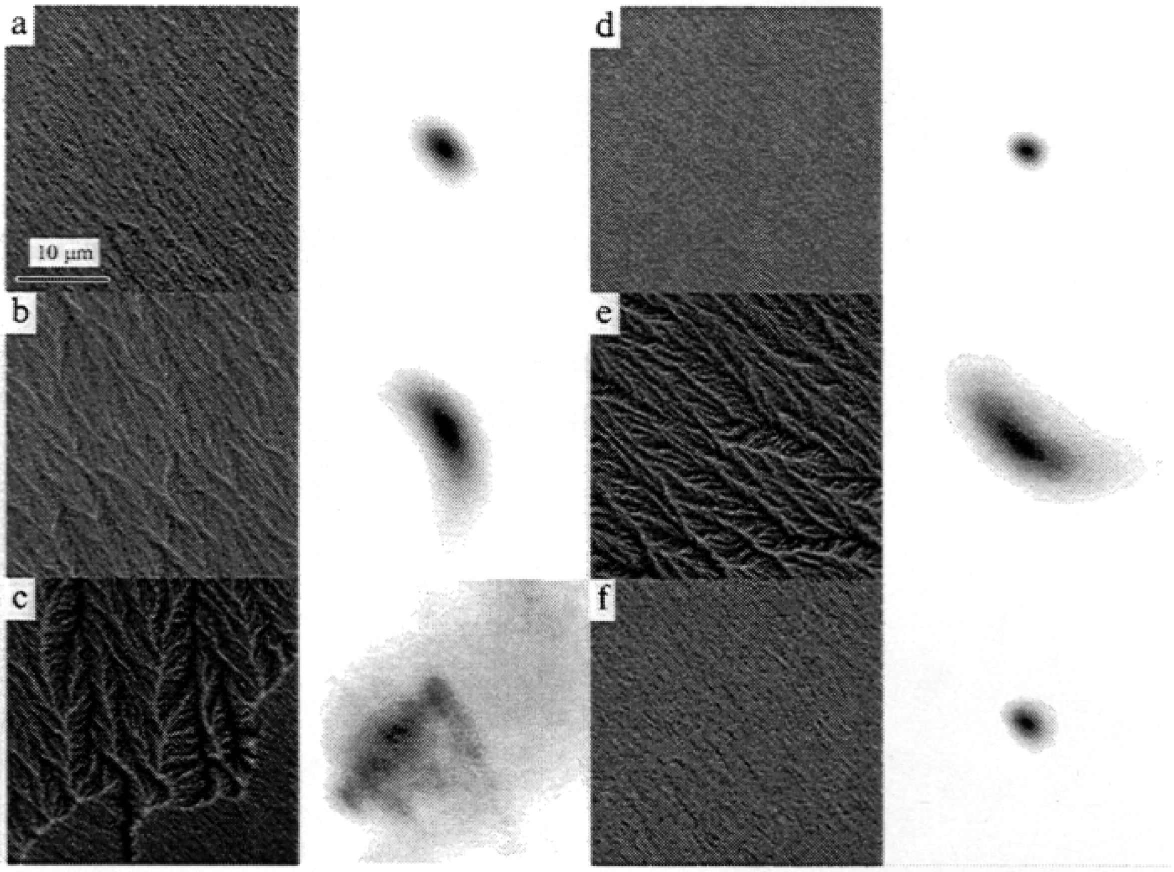

Fig. 4. Lorentz images and histograms of the magnetisation direction (as in fig. 3) as the Co film is taken through a hysteresis cycle. The field applied for each image is: a) 0, b) -2.6×10^{-3}, c) -2.8×10^{-3}, d) -6.7×10^{-3}, e) $+2.9\times10^{-3}$, and f) $+3.2\times10^{-3}$ T. Note that the magnetisation in c) is not recovered properly as there is a reversal of magnetisation across the image on a scale larger than the area of the image, thus making the corresponding histogram difficult to interpret.

At a large enough field the magnetisation reverses, as shown partially complete in fig. 4c and complete in fig. 4d. If the applied field is reversed again then the cycle repeats in the opposite direction (figs. 4e & f). For fig. 4c the magnetisation reversal between the top left and bottom right is on too large a scale to be reconstructed properly so the resulting histogram can no longer be interpreted easily.

4. Conclusion

The magnitude and direction of the magnetisation in a material can be recovered quantitatively from a Lorentz image knowing only the magnification, defocus and thickness. Although the method suffers from artefacts at low frequencies, it allows large areas away from the sample edge to be analysed rapidly and directly. We thank M.R. McCartney and D.J. Smith for discussions and for the NdFeB holography result. The images were obtained at the Center for High-Resolution Electron Microscopy at Arizona State University.

References

Chapman JN 1984, J. Phys. D **17**, 623
Cohen MS 1967, J. Appl. Phys. **38**, 4966
Cowley JM 1995, Diffraction Physics (3rd edition), North-Holland
Dunin-Borkowski RE, McCartney MR and Smith DJ 1998, Rec. Res. Dev. in Appl. Phys. **1**, 119
Paganin D and Nugent KA 1998, Phys. Rev. Lett. **80**, 2586
Tonomura A 1992, Adv. Phys. **41**, 59